EUMETSAT Satellite Application Facility on
Support to Operational Hydrology and Water Management
http://hsaf.meteoam.it/

Algorithm Theoretical Baseline Document (ATBD) H26

Soil Wetness Index in the roots region
by ASCAT soil moisture assimilation

Revision History

Revision	Date	Author(s)	Description
0.1	2019/07/24	David Fairbairn and Patricia de Rosnay	First draft.
0.2	2021/05/06	David Fairbairn and Patricia de Rosnay	Updated to include revised ASCAT bias correction (Sections 4.1.3 to 4.1.4) and description of postprocessing rescaling from volumetric to liquid wetness index (section 4.3.4)
0.3	2021/07/14	David Fairbairn and Patricia de Rosnay	Revised version after H26 ORR.

Table of Contents

List of Tables

List of Figures

List of Acronyms

ASAR Advanced Synthetic Aperture Radar (on Envisat)

ASAR GM ASAR Global Monitoring

ASCAT Advanced Scatterometer

ATBD Algorithm Theoretical Baseline Document

BUFR Binary Universal Form for the Representation of meteorological data

DORIS Doppler Orbitography and Radiopositioning Integrated by Satellite (on Envisat)

ECMWF European Centre for Medium-range Weather Forecasts

ERS European Remote-sensing Satellite (1 and 2)

ESA European Space Agency

EUMETCast EUMETSAT's Broadcast System for Environment Data

EUMETSAT European Organisation for the Exploitation of Meteorological Satellites

FTP File Transfer Protocol

H SAF SAF on Support to Operational Hydrology and Water Management

HTESSEL Hydrology Tiled ECMWF Scheme of Surface Exchanges over Land

LDAS Land Data Assimilation System

Météo France National Meteorological Service of France

Metop Meteorological Operational Platform

NRT Near Real-Time

NWP Numerical Weather Prediction

PRD Product Requirements Document

PUM Product User Manual

PVR Product Validation Report

SAF Satellite Application Facility

SEKF Simplified Extended Kalman Filter

SSM Surface soil moisture

SWI Soil Wetness Index

TU Wien Technische Universität Wien (Vienna University of Technology)

WARP Soil Water Retrieval Package

WARP H WARP Hydrology

WARP NRT WARP Near Real-Time

ZAMG Zentralanstalt für Meteorologie und Geodynamic (National Meteorological Service of Austria)

1. Executive summary

The Algorithm Theoretical Baseline Document (ATBD) provides a detailed description of the algorithm used to produce the near-real-time (NRT) H SAF scatterometer root zone soil moisture product (RZSM-ASCAT-NRT-10km/H26). The concept of the H26 production chain is based on scatterometer Surface Soil Moisture (SSM) data assimilation in a dedicated Land Data Assimilation System (LDAS) used to propagate the scatterometer surface soil moisture information in the vertical dimension to the root zone and in the time dimension at the daily time scale. The input information is the surface soil moisture derived from the Advanced scatterometer on-board Metop-A (ASCAT-A), Metop-B (ASCAT-B) and Metop-C (ASCAT-C). The H26 product assimilates these observations into the HTESSEL land surface model. It improves on its predecessor H14 through increased resolution (10 km instead of 25 km) and improved timeliness (12 hours instead of 36 hours). The processing chain is based on the ECMWF land surface model H-TESSEL (Hydrology Tiled ECMWF Scheme of Surface Exchanges over Land) constrained by ASCAT-derived SSM assimilation through the Simplified Extended Kalman Filter (SEKF).

The 10 km resolution H26 scatterometer root zone soil wetness index is available daily at the global scale with a timeliness of 12 hours i.e. it should arrive no later than 12 hours after the analysis time. It consists of a root zone soil wetness index profile, provided on four soil layers. It is relevant to operational hydrological applications (e.g. flood/drought prediction), water budget investigations and validation activities.

An introduction (section 2) to this document is followed by an introduction to the RZSM-ASCAT-NRT-10km (H26) product (section 3). The production chain is described in section 4 and the output data are illustrated in section 5. A conclusion is given in section 6. Section 7 provides scientific and technical references.

2. Introduction

2.1. Purpose of the document

The Algorithm Theoretical Baseline Document (ATBD) is intended to provide a detailed description of the scientific background and theoretical justification for the algorithms used to produce the NRT root-zone soil wetness index (H26).

2.2. Targeted audience

This document mainly targets:

- Hydrology and water management experts;
- Operational hydrology and Numerical Weather Prediction communities;
- Users of remotely sensed soil moisture for a range of applications (e.g. validation/benchmarking).

2.3. H SAF soil moisture products

In the framework of the H SAF project several soil moisture products, with different timeliness (e.g. near real time products and data records), spatial resolution, format (e.g. time series, swath orbit geometry, global image) or the representation of the water content in various soil

layers (e.g. surface, root-zone), are generated on a regular basis and distributed to users. A list of all available soil moisture products, as well as other H SAF products (such as precipitation or snow) can be looked up on the H SAF website (hsaf.meteoam.it). More general information about H SAF can be found in the Appendix. This document describes the production chain of the NRT H26 root zone soil wetness product.

3. Introduction to the NRT root-zone soil wetness index product

3.1. Principal of the product

The H26 production chain uses a sequential Land Data Assimilation System (LDAS) based on a Simplified Extended Kalman Filter (SEKF) method, as in [2]. The SEKF constitutes the central component of the H26 production chain. The H-TESSEL Land Surface Model is used to propagate in time and space the soil moisture information through the root zone, accounting for physiographic information (soil texture, orography), meteorological conditions and land surface processes such as soil evaporation and vegetation transpiration [3–5]. H26 is a root zone soil moisture product derived from Metop ASCAT-A/B/C surface soil moisture (SSM) observations. The retrieval approach relies on a sequential Land Data Assimilation System (LDAS) with 12-hour assimilation windows. The LDAS for H26 is implemented using the stand-alone surface analysis (SSA) configuration of [6]. The atmospheric analysis is forced from the archived operational 9 km ECMWF analysis, but the LDAS and coupled first guess are performed independently. Figure 3.1 illustrates the H26 production suite.

3.2. Main characteristics

H26 is a daily NRT product valid at 00UTC and with a timeliness of 12 hours i.e. the 00 UTC output should arrive on the H SAF ftp no later than 12 UTC. H26 is produced at a horizontal resolution of about 10km on four vertical layers in the soil: surface to 7 cm (layer 1), 7 cm to 28 cm (layer 2), 28 cm to 100 cm (layer 3), and 100 cm to 289 cm (layer 4). Whilst the 4th layer is provided it is not listed in the product requirements as there are no in situ reference observations available to validate soil moisture at this depth. H26 relies on a data assimilation approach that propagates the information in time and space (on the vertical dimension in the root zone). Therefore, it allows a global update of the root zone soil moisture states using SSM derived from the aforementioned ASCAT products. The soil moisture in the model and in the data assimilation process is in volumetric units. Prior to data assimilation, the SSM scatterometer derived observations are rescaled to match the model soil moisture climatology (described in Section 4.1.2) and in the process they are effectively converted to volumetric units. However, the H26 root-zone soil moisture product is expressed as a liquid soil wetness index, with units between 0 (zero soil moisture) and 1 (saturation), representing the lower and upper soil moisture limits. After data assimilation, a post-processing step is required to convert the volumetric soil moisture analysis into the soil wetness index (described in Section 4.4). It is computed using the soil texture (as defined by the FAO/United Nations Educational, Scientific and Cultural Organization (UNESCO) Digital Soil Map of the world [7]), the saturated soil moisture, and the fraction of liquid water content (the fraction of water that is not frozen) on each grid point and each soil layer. Having the units of H26 as a liquid soil wetness index is consistent with all the other ASCAT soil moisture products that are available for the surface

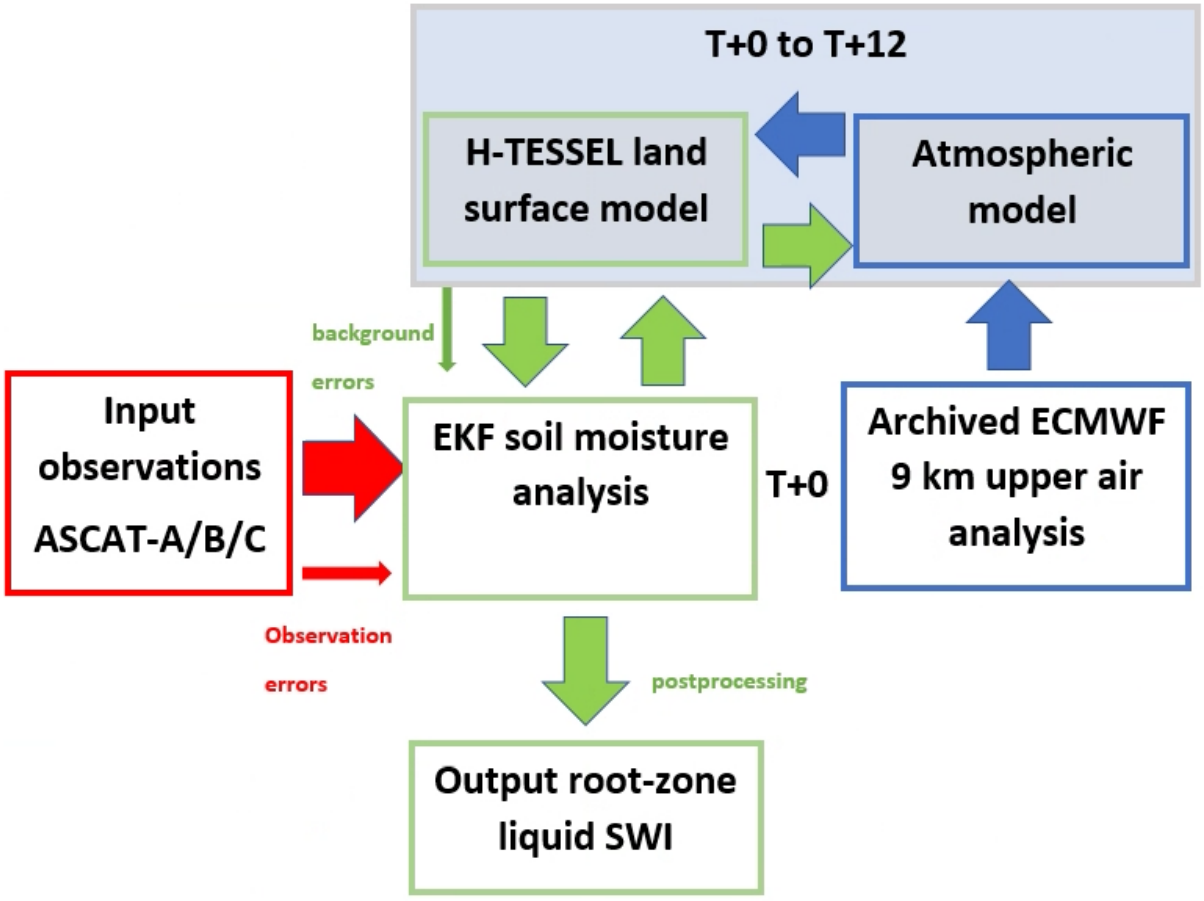

Figure 3.1: Illustration of the H26 root zone soil moisture production chain based on ASCAT-A/B/C satellite derived surface soil moisture data assimilation in the SSA configuration. The highlighted box encompasses the coupled land-atmosphere 12-hour first guess.

(e.g. H27 and H101). Furthermore, it is relevant to various applications and can be combined with different hydrological models (e.g. [8]).

The performance of H26 is firstly assessed by comparing the temporal correlation against ground measurements from the International Soil Moisture Network (ISMN[1], [9]). Additional metrics, including the anomaly correlation coefficient, the root-mean-square error and the bias are also considered. Data from 5 networks in the ISMN are considered for the validation. Three networks are located in the US: NRCS-SCAN (Natural Resources Conservation Service - Soil Climate Analysis Network), USCRN (U.S. Climate Reference Network) and NRCS-SNOTEL (short for Snow Telemetry) [10,11]. The SMOSMANIA (Soil Moisture Observing System Meteorological Automatic Network Integrated Application) network [12,13] is located over southwest France and the REMEDHUS network in Spain [14]. Secondly, a triple colocation analysis is used to assess the surface layer performance of H26, where the two other soil moisture products come from the NOAH Global Land Data Assimilation System (GLDAS, [15]) and the European Space Agency Climate Change Initiative (ESA CCI) passive soil moisture dataset [16]. Furthermore, the previous NRT product H14 is used as a benchmark to validate the performance of H26 over the June 2018 to May 2019 period. Table 3.1 presents the soil wetness index user requirements originally adopted in the H SAF Second Continuous Development and Operations Phase CDOP-2 and also used for the previous near-real-time (NRT) product (H14) and the H141 data record in the third development phase (CDOP-3). Details and results regarding the validation can be found in the Product Validation Report [17].

Table 3.1: Performance requirements for product H26 [CC]

Unit	Threshold	Target	Optimal
Dimensionless	0.5	0.65	0.8

3.3. Product uniqueness and heritage

The ECMWF H SAF dedicated LDAS has been operational since the First Continuous Development phase (starting in 2012) for the NRT H14 product and the second/third phase for the H27/H140 data record. It is run independently of the ECMWF operational system. The validations of these products have demonstrated that the LDAS is robust, reliable and that it provides high quality root zone soil wetness index fields.

H26 supersedes the original NRT product (H14), which was the first global product of consistent surface and root zone soil moisture available NRT for the NWP, climate and hydrological communities. H26 improves on H14 through increased resolution (25 to 10 km) and improved timeliness (12 hours instead of 36 hours). The H26 product employs a more recent version of the SEKF soil moisture analysis that was introduced in cycle 46r1 of the ECMWF/H SAF LDAS. This SEKF uses an ensemble of data assimilations (EDA) approach to provide flow-dependent observation operator Jacobians [18]. The EDA is produced using an ensemble of atmospheric 4D-Var data assimilation systems [19] and provides flow-dependent uncertainty information for both the atmosphere and the land surface. More detail on this SEKF formulation is provided in section 4.3. On the other hand, the original H14 product uses the previous formulation of the SEKF Jacobians, where the elements of the Jacobian matrix $\mathbf{H}$ are estimated by finite differ-

[1] https://ismn.geo.tuwien.ac.at/en/

ences [2]. The new Jacobian formulation is more efficient than the previous version and is able to capture the errors of the day through the EDA spread.

H26 is the first operational LDAS to be implemented using the SSA configuration (as illustrated in Figure 3.1), which was introduced and evaluated by [6]. SSA is a simplification of the weakly coupled land-atmosphere data assimilation (WCDA) approach used for H14 (described in [20]). Unlike WCDA, the atmospheric analysis in SSA is not performed explicitly, rather it is forced from an archived atmospheric analysis at the start of each cycle. Therefore, there is no feedback from the land to the atmospheric analysis. All other aspects of WCDA and SSA are the same. SSA is much faster than WCDA since it skips the expensive atmospheric 4D-Var analysis and preliminary evaluations suggest that the SM performance is comparable for the SSA and WCDA systems [6]. This reduction in computational cost enables H26 to be produced at higher resolution and improved timeliness compared with H14. It is expected that H14 will be discontinued about a year after H26 becomes operational (they will overlap for one year). It should be noted that SSA employs a coupled land-atmosphere prior forecast between assimilation cycles. This sets it apart from the offline LDAS employed in the H141 SM data record (1992-2018), where the land surface model is forced by the ERA-5 atmospheric reanalysis. The H14 and H141 production chains also assimilate screen-level variable (SLV) observations close to the surface (2-metre temperature and relative humidity). However, [6] found that assimilating these observations does not significantly impact the SM performance. Hence H26 only assimilates ASCAT-derived SSM observations. The main differences between the H26, H14 and the H141 production chains are summarized in Table 3.2.

Table 3.2: Differences between H26 (near-real-time), H14 (near-real-time) and H141 (data record) production chains. The * superscript implies that the observations were reprocessed from January 1992 to March 2014.

Product	H26 NRT	H14 NRT	H141 data record
Period	2021-present	2012-present	1992-2018
SSM observations	ASCAT-A/B/C	ASCAT-A/B	ERS 1/2* (1992-2006) and ASCAT-A/B* (2007-2018)
SLV assimilation	No	Yes	Yes
DA system	Regular updates of LDAS (47R2-)	Regular updates of LDAS (38R1 - 47R2)	Fixed LDAS cycle 46R1
LDAS config.	SSA	WCDA	Offline (ERA-5 forcing)
Resolution	10 km	25 km	10 km

4. Production chain

The main components of the H26 production as presented in Figure 3.1 are detailed hereafter. They include the input data and reprocessing, which includes a recalibration of the ASCAT bias correction parameters. The H-TESSEL land surface model and the SEKF data assimilation system are then explained, followed by the post-processing.

4.1. Input data and reprocessing

4.1.1. Remotely sensed soil moisture

Table 4.1 below gives the details on the ASCAT-A/B/C SSM products used as input of the H26 production suite. Note that the ASCAT-A satellite is planned to be decommissioned in November 2021.

Table 4.1: Scatterometer SSM products used in the NRT H26 product. N.A. stands for "not applicable".

Sensor	Producer	Reference
ASCAT-A (until Nov 2021), ASCAT-B and ASCAT-C 25 km sampling	EUMETSAT CAF	ASCSMO02: ASCAT-A/B/C 25 km swath grid product distributed by CAF. (https://vnavigator.eumetsat.int/product/EO:EUM:DAT:METOP:SOMO25). Equivalent to H SAF level 2 surface soil moisture products H102 (Metop-A 25 km sampling), H103 (Metop-B 25 km sampling) and H105 (Metop-C 25 km sampling).

A quality control is applied to filter ASCAT SSM observations so that only observations with a noise level lower than 15% are used for H26. The quality control also rejects ASCAT SSM observations for pixels with a water fraction larger than 15% and with a topographic complexity larger than 20%, as well as observations in frozen soil and/or snow covered surface conditions. A processing flag filters out ASCAT observations that are considered to be corrupted.

4.1.2. Rescaling

Biases between the spectrometer-derived soil moisture data and the model need to be removed prior to data assimilation [21–23]. Each soil moisture data set is characterized by its specific mean value, variability and dynamical range. The HTESSEL land surface model has its own soil moisture climatology with a specific dynamical range controlled by the values at the wilting point and field capacity (functions of soil textural types). The approach described in [21] (using a simplified form of a Cumulative Distribution Function, CDF) is used here. It is a linear rescaling technique designed to match the climatological mean and variance of the scatterometer level 2 observations with the HTESSEL soil moisture. The global CDF matching parameters A and B are computed individually for each model gridpoint over a specified calibration period as follows:

$$\begin{aligned} A &= \overline{\theta}_m - B \times \overline{\theta}_o \\ B &= \frac{\sigma_m}{\sigma_o}, \end{aligned} \tag{1}$$

where $\overline{\theta}_m$ and $\overline{\theta}_o$ stand for the means of model and observation surface soil moisture, respectively, while σ_m and σ_o represent the standard deviations of model and observations, respectively.

A CDF matching version which accounts for seasonal variability was implemented by [24, 25] and has been adopted in the ECMWF/H SAF SM analysis since the H14 production [20]. The CDF matching parameters are derived for each calendar month using a similar approach to [26]

for passive microwave data, which employs a 3-month moving average. For example, for the month of May the parameters are derived based on the data from April, May and June over a multi-year calibration period.

4.1.3. Recalibrating the bias correction parameters

The CDF matching bias correction should be updated regularly to account for calibration changes in the input observations and small changes in the land surface model. The original bias correction used in the H SAF root-zone SM production suites is based on ERS/SCAT (2000-2006), ASCAT-A (2007-2009) and H-TESSEL forced by ERA-Interim atmospheric conditions over a 10-year period (2000-2009). Recently, the ERA-interim reanalysis has been superseded by ERA5 [27], which is closer to the current H SAF/ECMWF operational cycle (cycle 47r2 in May 2021). The development of H26 provided an opportunity to re-calibrate the CDF matching parameters based on ASCAT-A/B derived SM and ERA5 surface SM over a recent period (2009-2018).

4.1.4. H26 CDF matching performance

An evaluation was performed by comparing the differences between the HTESSEL SM with the ASCAT-A/B SM before and after bias-correction, over the 2019 calendar year. The HTESSEL SM comes from an offline run of the ECMWF/ HSAF HTESSEL model forced by ERA5 atmospheric fields. Table 4.2 summarises the statistics for the ASCAT and HTESSEL SM integrated over the global domain. CDFH14 rescales the ASCAT SM using the H14 CDF matching parameters and CDFH26 rescales the ASCAT SM using the new CDF matching parameters. As expected, prior to rescaling, the ASCAT SM index has a much higher mean, standard deviation, minimum and maximum than the HTESSEL SM. The ASCAT CDFH14 statistics are closer to the HTESSEL SM than the ASCAT index, although they are all slightly over-estimated. The mean SM, minimum and maximum are less biased with respect to HTESSEL after applying the new CDF matching (CDFH26). The same statistics integrated over Europe is shown in Tables 4.3. The ASCAT CDFH14 has a higher mean SM compared to HTESSEL and the ASCAT CDFH26 has a slightly lower mean than HTESSEL, but the gap is smaller with CDFH26. Figure 4.1 shows a time series plot of surface SM integrated over Europe for ASCAT after rescaling, as well as the HTESSEL SM. Evidently the CDFH14 rescaled ASCAT SM has a positive bias with respect to HTESSEL during the summer period (Figure 4.1a), but the bias is not present in the CDFH26 rescaled ASCAT SM (Figure 4.1b). Importantly, the short-term signal in the ASCAT dataset is not modified by the bias-correction.

Table 4.2: Statistics of ASCAT data, the HTESSEL SM, ASCAT after CDF matching with the current parameters (CDFH14) and after rescaling with the new parameters (CDFH26), averaged over the global domain over 2019.

	Min	Max	Mean	Std
ASCAT index (-)	0.288	0.572	0.404	0.079
HTESSEL (m3/m3)	0.195	0.284	0.238	0.021
ASCAT CDFH14 (m3/m3)	0.202	0.300	0.254	0.024
ASCAT CDFH26 (m3/m3)	0.194	0.278	0.235	0.019

Table 4.3: Same as Table 4.2 but over Europe.

	Min	Max	Mean	Std
ASCAT index (-)	0.12	0.90	0.42	0.17
HTESSEL (m3/m3)	0.15	0.42	0.29	0.06
ASCAT CDFH14 (m3/m3)	0.17	0.44	0.31	0.06
ASCAT CDFH26 (m3/m3)	0.12	0.43	0.28	0.06

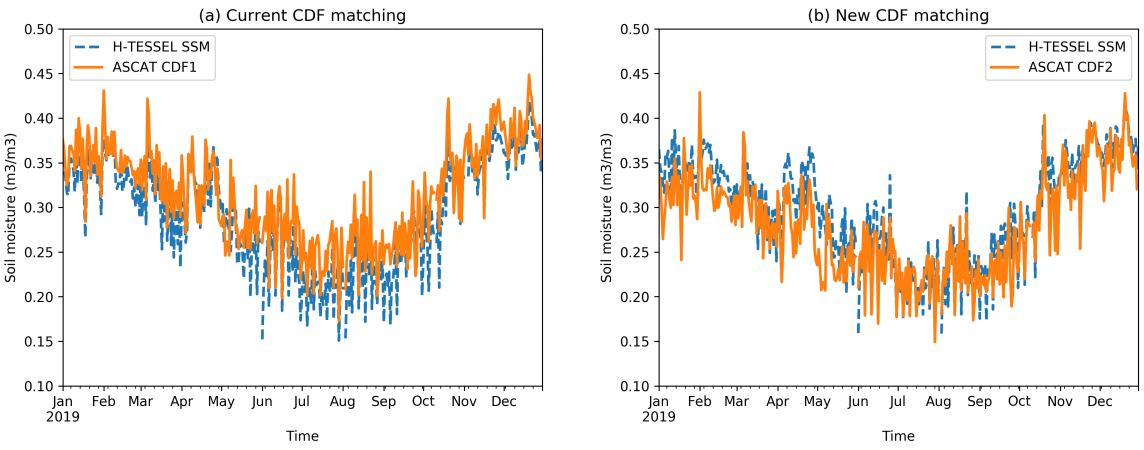

Figure 4.1: Surface SM time series for 2019, integrated over Europe, for (a) ASCAT CDFH14 (labelled CDF1) (m3/m3) and HTESSEL SM (m3/m3); (b) same as (a) but with ASCAT CDFH26 (labelled CDF2) instead of CDFH14.

4.2. The H-TESSEL land surface model

In the H26 production chain, the temporal and vertical propagation of soil moisture from the surface soil towards the root zone is driven by the H-TESSEL land surface model [3–5]. The H-TESSEL formulation of the soil hydrological conductivity and diffusivity accounts for spatial variability according to a global soil textural map [7]. A monthly leaf area index (LAI) climatology is used based on a MODIS satellite product as described in [28]. Surface runoff is based on the variable infiltration capacity. The soil heat budget follows a Fourier diffusion law, modified to take into account soil water freezing/melting according to [29]. The energy equation is solved with a net ground heat flux as the top boundary condition and a zero flux at the bottom. The water balance at the surface (i.e., the change in water storage of the soil moisture, interception reservoir, and accumulated snowpack) is computed as the difference between the precipitation and (i) the evaporation of soil, vegetation, and interception water and (ii) surface and subsurface runoff. First precipitation is collected in the interception reservoir until it saturated. Then, excess precipitation is partitioned between surface runoff and infiltration into the soil column. Bare ground evaporation over dry land uses a lower stress threshold than for the vegetation, allowing a higher evaporation [30]. This is in agreement with the modelled findings of [31] and results in more realistic soil moisture for dry land [32].

4.3. Extended Kalman filter

A point-wise SEKF is used to assimilate scatterometer surface soil moisture to produce the root zone soil moisture, which is converted afterwards into the H26 soil wetness index. The SEKF constitutes the core of the H26 production chain. On each grid point the analysis update equation of the SEKF is expressed as:

$$\mathbf{x}^a(t_i) = \mathbf{x}^b(t_i) + \mathbf{K}_i(\mathbf{y}^o(t_i) - h(\mathbf{x}^b(t_i))), \tag{2}$$

where $\mathbf{x}$ is the control state vector which is the vertical soil moisture profile for the n analysed layers of the land surface model. The number of observations assimilated has dimension p. $\mathbf{B}$ is the background error covariance matrix (of dimension n times n), $\mathbf{R}$ is the observation error covariance matrix (of dimension p times p). The "a", "b" and "o" superscripts denote analysis, background and observation, respectively. Transpose matrices are indicated by the superscript T. The Kalman gain $\mathbf{K}$ determines the weight to give to the background and the observations:

$$\mathbf{K}_i = [\mathbf{B}^{-1} + \mathbf{H}_i^T\mathbf{R}^{-1}\mathbf{H}_i]^{-1}\mathbf{H}_i^T\mathbf{R}^{-1}, \tag{3}$$

Flow-dependent background-error covariances are implicitly provided via the observation operator Jacobians (equation (5) in Section 4.3.1). The observation operator is denoted by h, which transforms the model control variables into the observation space at the observation time (t_i). In the H26 production chain, n=3, with the top three layers being analysed. $\mathbf{y}^o$ is the observation vector which contains p observations of surface soil moisture scatterometer observations available within the data assimilation window. The ASCAT-derived SSM observations are assimilated at the nearest 15 minute timestep. The observation operator h allows the computation of the model counterpart of the observations. The linearized observation operator $\mathbf{H}$ is a matrix of dimension n times p and each element in $\mathbf{H}$ is a Jacobian representing the tangents of the observation operator at the observation times. The nonlinear model M propagates the analysis

forwards in time from one timestep to the next:

$$\mathbf{x}^b(t_{i+1}) = M(\mathbf{x}^a(t_i)) \tag{4}$$

4.3.1. Jacobian matrix

The elements of the Jacobian matrix **H** are estimated using the EDA ensemble spread (see [19] for information on the EDA). In previous cycles of the ECMWF/H SAF LDAS (from 2010 to 2019) the Jacobians were calculated using finite differences. The new approach using the EDA ensemble is advantageous over the finite difference approach for two reasons [18]: Firstly, it delivers computational savings since the EDA is already computed in the ECMWF operational system. Secondly, it offers improved land-atmosphere coupling compared with the finite difference approach, since the errors of the day are propagated from one cycle to the next. An article introducing and evaluating the EDA Jacobians implementation in the SEKF is currently being written (Patricia de Rosnay, personal communication).

The covariances between the model predicted values of the ASCAT observations (represented by the first SM layer) and the SM prognostic variables are calculated and divided by the variances of the SM prognostic variables. The EDA formulation is documented for the latest IFS cycle [33]. The Jacobian linking the i^{th} element of the ASCAT SM observation to soil moisture index layer j of the model state vector is given by:

$$\mathbf{H}_{i,j} = \frac{cov(H_i(\mathbf{x}^{eda}), \mathbf{x}_j^{eda})}{var(\mathbf{x}_j^{eda})}.c_j \tag{5}$$

where "cov" and "var" stand for "Covariance" and "Variance" respectively and *eda* indicating that the EDA ensemble fields are used. Also, the tapering coefficient is given by $c_j = 1/(1 + (j-1).\alpha_{sekf})$, where $\alpha = 0.6$. This coefficient is empirically derived and reduces the size of the Jacobians at depth.

The elements of the Jacobian matrix are governed by the physics of the model. Their examination is important to understand the data assimilation system performances [34]. From equation (5) the Jacobians for the first layer are equal to 1.0, but the Jacobians for the other layer depend on the vertical covariances. As illustrated by the histograms of Figure 4.2 for one site located in southwest France (corresponding to the Saint Felix station of the SMOSMANIA network, 43.44°N/1.88°E) over June to August 2018, the sensitivity of SSM to changes in soil moisture of the first layer of soil is higher than that of the second and third layers of soil (Figure 4.2 a, b and c, respectively). Therefore, the assimilation system will be more effective in modifying soil moisture from the first layer.

4.3.2. Error specifications

The description of the error matrices is a key aspect of data assimilation [35,36]. The correction of the system state depends on the background and observation error specifications. The soil moisture observation-error covariance matrix **R** is homogeneous and diagonal with standard deviations of $0.02\text{m}^3/\text{m}^3$ (as in [2]). The background error covariance matrix **B** is also a diagonal matrix with standard deviations of $0.01\text{m}^3/\text{m}^3$. Whilst the prescribed ASCAT observation errors are larger than the background errors, they are small enough for the observations to significantly impact the SM state over many parts of the world [2].

(a) $\frac{\delta SML1}{\delta SML1}$ histogram

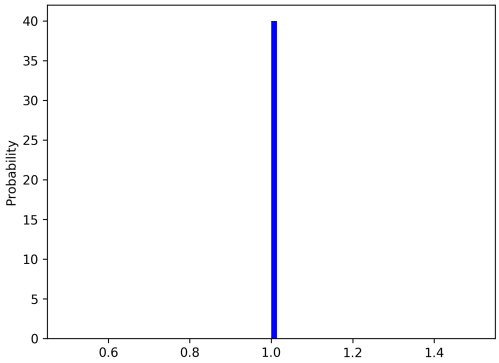

(b) $\frac{\delta SML1}{\delta SML2}$ histogram

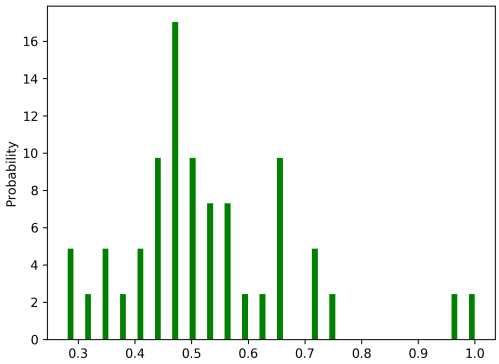

(c) $\frac{\delta SML1}{\delta SML3}$ histogram

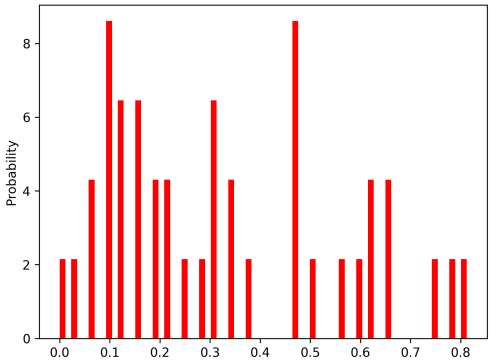

Figure 4.2: Illustration of EDA Jacobians for one site located in the France (corresponding to the station Saint Felix of the SMOSMANIA network, 43.44°N/1.88°E), The histograms of the Jacobians of SSM to perturbations in soil moisture layers 1, 2 and 3 are shown in Figures (a), (b) and (c) respectively.

4.3.3. Early delivery suite

The H26 product is produced independently of the ECMWF operational system, but using the same "early delivery" configuration in the IFS. The "early delivery" concept is detailed in [1] and illustrated in Figure 4.3. Two 12-hour assimilation windows are performed, from 2100 to 0900 UTC and from 0900 to 2100 UTC. The SEKF long-window analysis is performed over the same 12-hour assimilation window as the operational ECMWF atmospheric 4D-Var analysis [2]. These analyses are run with a delayed-cut-off time, in order to use the maximum possible number of observations. The extraction tasks for observations in the periods 21:01 - 03:00 UTC and 03:01-09:00 UTC are run at 13:45 and 14:00 UTC respectively, while the extraction tasks for observations in the periods 09:01 - 15:00 UTC and 15:01-21:00 UTC are run at 01:45 and 02:00 UTC, respectively.

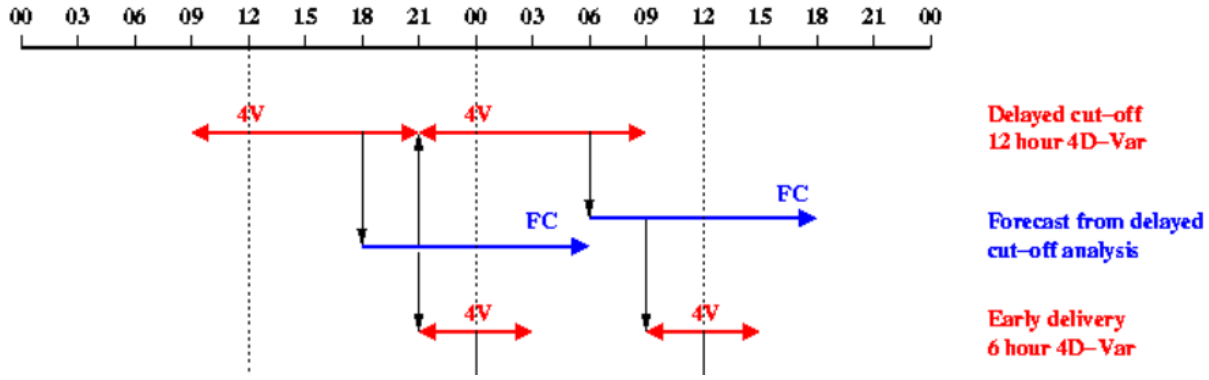

Figure 4.3: Early delivery configuration of the operational ECMWF IFS [1]. H26 adopts the same configuration for the SEKF SM analyses and the first guess forecasts, but the atmospheric 4D-Var analyses are instead read in from the high resolution operational archive.

The early-delivery analyses were originally introduced to make the ECMWF operational products available earlier. For the purposes of the H SAF NRT SM products an early delivery analysis has also been adopted, since it substantially improves the timeliness of the products. These early delivery analyses do not propagate information from cycle to cycle. Each analysis is reinitialized with the best available model fields from the delayed-cut-off assimilation.

In the ECMWF operational setup, the 00:00 UTC early-delivery analysis is a 6-hour 4D-Var analysis that uses observations in the window 21:01-03:00 UTC. The cut- off time is 04:00 UTC, and any observations that arrive after this time are not used by the early-delivery analysis. The first guess for the 00 UTC early-delivery analysis is the nine-hour forecast from the previous day's 12 UTC delayed-cut-off 12-hour 4D-Var analysis. The 12:00 UTC early-delivery analysis is a 6-hour 4D-Var analysis that uses observations in the window 09:01-15:00 UTC. The cut-off time is 16:00 UTC. The first guess for the 12:00 UTC early-delivery analysis is the nine-hour forecast from the 00:00 UTC delayed-cut-off 12-hour 4D-Var analysis. The early delivery SEKF SM analysis follows the same assimilation window as the 4D-Var.

H26 is implemented in the "early delivery" configuration with the SSA system [6]; hence the atmospheric analysis is not performed explicitly, rather the atmospheric fields are forced from the archived operational ECMWF atmospheric analysis. This ensures that the 00 UTC SEKF early delivery SM analysis is performed quickly enough to meet the timeliness of 12 hours.

4.4. Post-processing

The soil moisture is expressed in volumetric units in the model and data assimilation. Three post-processing steps are required to convert the soil moisture analysis from volumetric units to a liquid soil wetness index (SWI):

1. Approximation of frozen fraction (F) of soil moisture (SM) below the field capacity. It is assumed that when the soil layer is below -3°C SM is completely frozen and above 1°C the SM is completely non-frozen. In between -3°C and 1°C the frozen fraction is calculated according to a linear relationship:

$$f = \frac{1 - T_{soil}}{4}, \tag{6}$$

   where T is the temperature of the soil (in °C).

2. Approximation of the liquid volumetric soil moisture. It is assumed that only water below the field capacity (SM_{cap}) can be frozen i.e. all water above the field capacity is non-frozen. If the SM is below the field capacity, the liquid soil moisture is simply calculated as:

$$SM_{liq} = SM - SM_{cap} + (1 - f) \times SM_{cap} = SM - f \times SM_{cap} \tag{7}$$

3. Conversion of liquid soil moisture to liquid soil wetness index (SWI):

$$SWI = \frac{SM_{liq}}{SM_{sat}}, \tag{8}$$

   where SM_{sat} is the soil moisture at saturation. Note that the parameters (SM_{cap}, SM_{sat}) are approximated based on the soil texture and vary depending on the fraction of clay, sand and loam in the soil. The SWI is bounded by (0,1), where 0 corresponds to the lower physical limit and 1 is the saturation point of the soil.

5. Output data

5.1. H26 production chain output data

The H26 output has 5 variables (i) soil wetness index analysis for each of the 4 layers; (ii) a quality control flag, which identifies gridpoints with soil wetness index values outside the nominal range (i.e. less than 0 or greater than 1), or where any layer has a soil temperature below 4°C i.e. there is a risk of frozen conditions. The quality control flag has one of 3 values for each gridpoint:

- 1 = normal
- 2 = risk of frozen conditions (one of the layers has a soil temperature less than 4°C)
- 3 = outside nominal range.

By design the SWI should always be in the nominal range (0-1), but a check is performed in case of corrupted data. However, many mountainous and high latitude regions are frozen, especially

in winter. This can be useful to link very low liquid SWI values with frozen conditions. Note that a value outside the nominal range (labelled 3) would always override a frozen value (2).

The H26 output data are provided at approximately 10 km resolution in two different formats in order to cater for the needs of different users. The model and data assimilation are performed on a cubic octahedral reduced Gaussian grid, which has approximately equidistant grid points between the equator and the poles. For each date a single GRIB file is provided of the soil moisture analysis in the original reduced Gaussian grid format, giving four fields of global soil wetness index (one for each soil layer). Additionally, the same fields are provided as a single netCDF file in a regular lat/lon format (created by interpolating the reduced Gaussian grid into a regular lat/lon grid). A more detailed description of the data format and structure can be found in the H26 Product User Manual [37].

5.2. Example of H26 output data

Figures 5.1 and 5.2 are H26 previews for 2 days; 01 June 2018 and 31 December 2018 respectively. The four layers of H26 are represented (0-7 cm, 7-28 cm, 28-100 cm and 100-289 cm from top to bottom). Note that only the first three layers are analyzed. As H26 represents the liquid part of the surface and root zone soil wetness index, one may notice that in winter (Figure 5.2) the high latitude northern areas (affected by snow and cold temperatures) share the same colour code as dry areas (e.g. the Sahara desert in Africa).

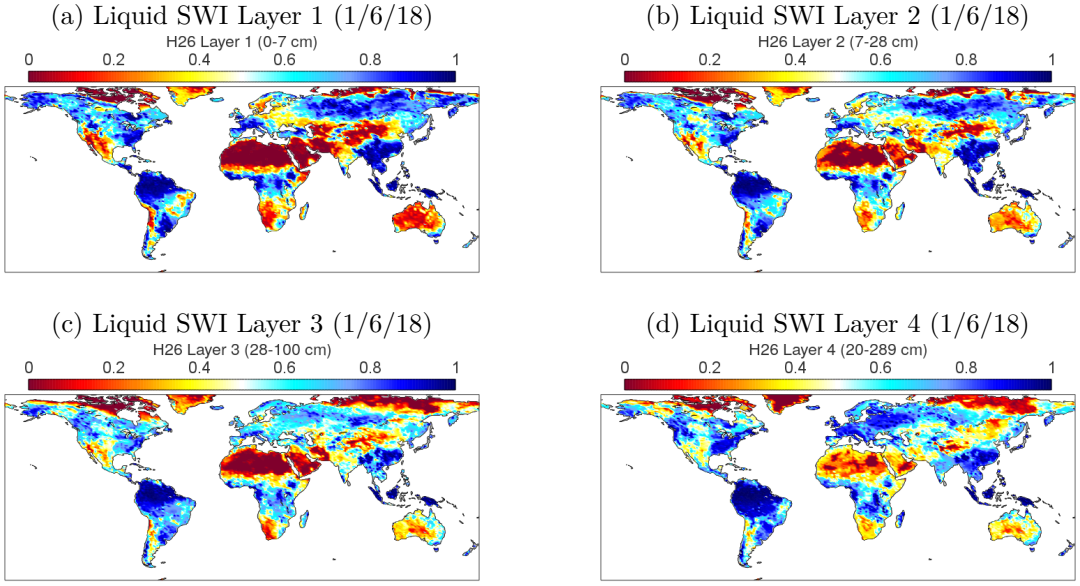

Figure 5.1: H26 previews for 01 June 2018 for the 4 layers of soil: (a) 0-7 cm, (b) 7-28 cm, (c) 28-100 cm and (d) 100-289 cm.

6. Conclusion

The RZSM-ASCAT-NRT-10km (H26) NRT product consists of a unique global scatterometer derived root zone soil wetness index, which is computed on a daily basis. The product results from

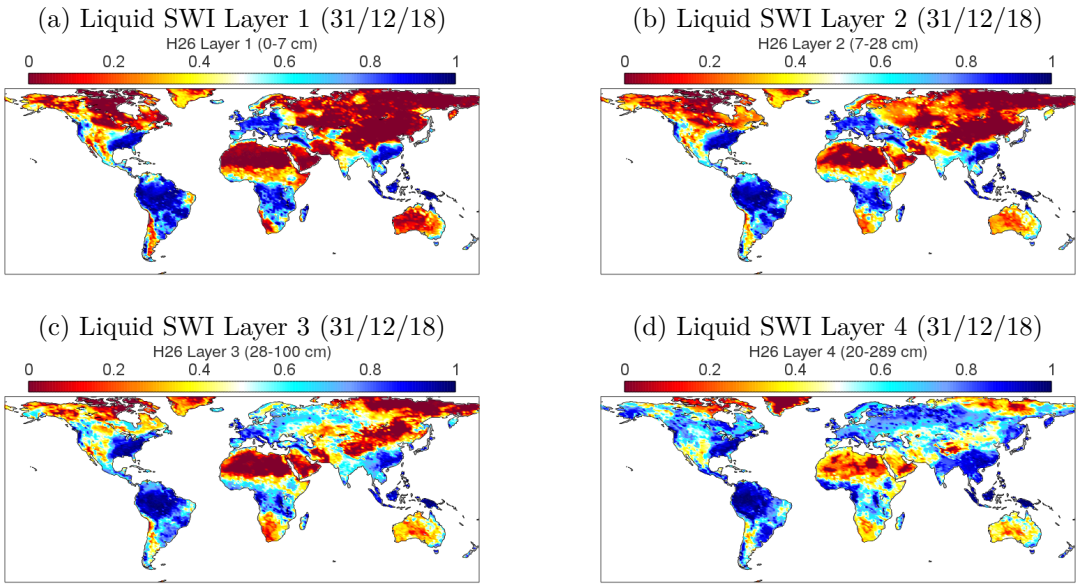

Figure 5.2: Same as Figure 5.1 but for 31/12/2018.

data assimilation which enables the propagation of the surface soil moisture information observed by scatterometers (ASCAT-A/B/C) to the root zone, taking into account land-atmosphere coupling in the forecast model. It improves on the original NRT root-zone product (H14) through reduced timeliness (12 hours instead of 36 hours) and increased resolution (10 km instead of 25 km). It is implemented using the early delivery suite of the ECMWF IFS and using the SSA configuration (i.e. the atmospheric analysis is forced rather than performed explicitly). H26 also assimilates ASCAT-C observations in addition to ASCAT-A/B and benefits from a recent recalibration of the ASCAT soil moisture bias correction parameters. H26 is expected to provide benefits for a range of hydrological research and operational activities.

The 10 km resolution H26 product is provided daily as a soil wetness index across the four root-zone layers. More information about the output format and visualizations of H26 can be found in the H26 product user manual [37]. A comprehensive validation of H26 against in situ measurements and a triple colocation validation can be found in the product validation report [17].

7. References

[1] J. Haseler, "Early–delivery suite," in *Technical Memorandum 454.* ECMWF, 2004, [Available online at http://www.ecmwf.int/publications/.].

[2] P. de Rosnay, M. Drusch, D. Vasiljevic, G. Balsamo, C. Albergel, and L. Isaksen, "A simplified Extended Kalman Filter for the global operational soil moisture analysis at ECMWF," *Quart. J. Roy. Meteor. Soc.*, vol. 139, pp. 1199–1213, 2013.

[3] B. van den Hurk, P. Viterbo, A. Beljaars, and A. Betts, "Offline validation of the ERA-40 surface scheme," in *Technical Memorandum 295.* ECMWF, 2000, [Available online at http://www.ecmwf.int/publications/.].

[4] B. van den Hurk and P. Viterbo, "The Torne-Kalix PILPS 2(e) experiment as a test bed for modifications to the ECMWF land surface scheme," *Global and Planetary Change*, vol. 38, pp. 165–173, 2003.

[5] G. Balsamo, A. Beljaars, K. Scipal, P. Viterbo, B. van den Hurk, M. Hirschi, and A. Betts, "A Revised Hydrology for the ECMWF Model: Verification from Field Site to Terrestrial Water Storage and Impact in the Integrated Forecast System," *J. Hydrometeor.*, vol. 10, pp. 623–643, 2009.

[6] D. Fairbairn, P. de Ronsay, and P. Browne, "The new stand-alone surface analysis at ECMWF: Implications for land-atmosphere DA coupling," *J. Hydrometeor.*, vol. 20, pp. 2032–2042, 2019.

[7] FAO, ""Digital soil map of the world (DSMW)"," in *Technical report.* Food and Agriculture organization of the United Nations, 2003.

[8] C. Massari, L. Brocca, L. Ciabatta, T. Moramarco, G. S., C. Albergel, P. De Rosnay, S. Puca, and W. Wagner, "The use of H-SAF soil moisture products for operational hydrology: flood modelling over Italy," *Hydrology*, vol. 2, pp. 2–22, 2015.

[9] W. Dorigo, W. Wagner, R. Hohensinn, S. Hahn, C. Paulik, A. Xaver, A. Gruber, M. Drusch, S. Mecklenburg, P. Oevelen, and A. Robock, "The International Soil Moisture Network: a data hosting facility for global in situ soil moisture measurements," *Hydrol. Earth Syst. Sci.*, vol. 15, pp. 1675–1698, 2011.

[10] G. Schaefer, M. Cosh, and T. Jackson, "The USDA natural resources conservation service soil climate analysis network (SCAN)," *J. Atmos. Oceanic Technol.*, vol. 24(2), pp. 2073–2077, 2007.

[11] J. E. Bell, M. A. Palecki, C. Baker, W. Collins, J. Lawrimore, R. Leeper, M. Hall, J. Kochendorfer, T. Meyers, T. Wilson, and H. Diamond, "U.S. Climate Reference Network soil moisture and temperature observations," *J. Hydrometeor.*, vol. 14, pp. 977–988, 2013.

[12] J. Calvet, N. Fritz, F. Froissard, D. Suquia, A. Petitpa, and B. Piguet, "In situ soil moisture observations for the CAL/VAL of SMOS: the SMOSMANIA network." in *Geoscience and Remote Sensing Symposium, IGARSS 2007.*, vol. 16 (3). IEEE International, 2007, pp. 1293–1314.

[13] C. Albergel, C. Rudiger, T. Pellarin, J.-C. Calvet, N. Fritz, F. Froissard, D. Suquia, A. Petitpa, B. Piguet, and E. Martin, "From near-surface to root-zone soil moisture using an exponential filter: an assessment of the method based on in situ observations and model simulations," *Hydrol. Earth Syst. Sci.*, vol. 12, pp. 1323–1337, 2008.

[14] N. Sanchez, J. Martinez-Fernandez, A. Scaini, and C. Perez-Gutierrez, "Validation of the SMOS L2 soil moisture data in the REMEDHUS network (Spain)," *IEEE Trans. Geosci. Remote Sens.*, vol. 50, pp. 1602–1611, 2012.

[15] M. Rodell, P. Houser, U. Jambor, J. Gottschalck, K. Mitchell, C.-J. Meng, K. Arsenault, B. Cosgrove, J. Radakovich, M. Bosilovich, J. Entin, J. Walker, and D. Lohmann, "The global land data assimilation system," *Bulletin of the American Meteorological Society*, vol. 85, pp. 381–394, 2004.

[16] A. Wagner, A. Dorigo, R. de Jeu, D. Fernandez, J. Benveniste, E. Haas, and M. Ertl, "Fusion of active and passive microwave observations to create an essential climate variable datarecord on soil moisture," in *In Proceedings of the XXII International Society for Photogrammetry and Remote Sensing (ISPRS) Congress*. Melbourne, Australia, 2012.

[17] "Product validation report (PVR), RZSM-ASCAT-NRT-10km (H26)," Tech. Rep. Doc. No: SAF/HSAF/PVR-26, v0.1, 2021.

[18] P. de Rosnay, "Coupled land-atmosphere data assimilation," in *ECMWF Data Assimilation training course*. Reading, UK: ECMWF, 2019, [Available online at https://confluence.ecmwf.int/display/OPTR/Data+Assimilation.].

[19] M. Bonavita, L. Isaksen, and E. Hólm, "On the use of EDA background error variances in the ECMWF 4D–Var," *Quart. J. Roy. Meteor. Soc.*, vol. 138(667), pp. 1540–1559, 2015.

[20] ATBD, "H14: Algorithm Theoretical Baseline Document, Soil Wetness Index in the roots region, Data Record," in *H14 ATBD*. H SAF, 2011, [Available online at http://hsaf.meteoam.it/user-documents.php.].

[21] D. M. Scipal, K. and W. Wagner, "Assimilation of a ERS scatterometer derived soil moisture index in the ECMWF numerical weather prediction system," *Adv. Water Resour.*, vol. 31, 2008.

[22] R. Reichle and R. Koster, "Bias reduction in short records of satellite soil moisture," *Geophys. Res. Lett.*, vol. 31, p. L19501, 2004.

[23] M. Drusch, E. F. Wood, , and H. Gao, "Observations operators for the direct assimilation of TRMM microwave imager retrieved soil moisture," *Geophys. Res. Lett.*, vol. 32, p. L15403, 2005.

[24] C. S. Draper, J.-F. Mahfouf, and J. Walker, "An EKF assimilation of AMSR-E soil moisture into the ISBA land surface scheme," *J. Geophys. Res.*, vol. 114, p. D20104, 2009.

[25] A. Barbu, J.-F. Calvet, J.-C. Mahfouf, and S. Lafont, "Integrating ASCAT surface soil moisture and GEOV1 leaf area index into the SURFEX modelling platform: a land data assimilation application over France." *Hydrol. Earth Syst. Sci.*, vol. 18, pp. 173–192, 2014.

[26] P. de Rosnay, J. Muñoz Sabater, C. Albergel, L. Isaksen, S. English, M. Drusch, and J.-P. Wigneron, "SMOS brightness temperature forward modelling and long term monitoring at ECMWF," *Remote Sens. Environ.*, vol. 237, 2020.

[27] H. Hersbach, B. Bell, P. Berrisford, A. Horanyi, J. Muñoz Sabater, J. Nicolas, R. Radu, D. Schepers, A. Simmons, C. Soci, and D. Dee, "Global reanalysis: goodbye ERA-Interim, hello ERA5," in *Newsletter No. 159*. ECMWF, 2019, [Available online at https://www.ecmwf.int/sites/default/files/elibrary/2019/19001-newsletter-no-159-spring-2019.pdf.].

[28] S. Boussetta, G. Balsamo, A. Beljaars, T. Kral, and L. Jarlan, "Impact of a satellite–derived leaf area index monthly climatology in a global numerical weather prediction model," *Int. J. Remote Sens.*, vol. 34(9-10), pp. 3520–3542, 2013.

[29] P. Viterbo and A. Beljaars, "An improved land surface parameterization scheme in the ECMWF model and its validation," *J. Climate*, vol. 8, 1995.

[30] C. Albergel, P. De Rosnay, C. Gruhier, J. Muñoz Sabater, S. Hasenauer, I. L., Y. Kerr, and W. Wagner, "Evaluation of remotely sensed and modelled soil moisture products using global ground–based in situ observations," *Remote Sens. Environ.*, vol. 118, pp. 215–226, 2012.

[31] J.-F. Mahfouf and J. Noilhan, "Comparative study of various formulations of evaporation from bare soil using in situ data," *J. Appl. Meteorol.*, vol. 30, pp. 351–362, 1991.

[32] Balsamo, G. and Boussetta, S. and Dutra, E. and Beljaars, A. and Viterbo, P. and van den Hurk, B., "Evolution of land surface processes in the IFS," *ECMWF Newsletter*, vol. 127, pp. 17–22, 2011.

[33] ECMWF, "IFS documentation," in *ECMWF website*. ECMWF, 2021, [Available online at https://www.ecmwf.int/en/forecasts/documentation-and-support/changes-ecmwf-model/ifs-documentation.].

[34] A. L. Barbu, J.-C. Calvet, J.-F. Mahfouf, C. Albergel, and S. Lafont, "Assimilation of Soil Wetness Index and Leaf Area Index into the ISBA-A-gs land surface model: grassland case study," *Biogeosciences*, vol. 19, pp. 1971–1986, 2011.

[35] W. T. Crow and R. H. Reichle, "Comparison of adaptive filtering techniques for land surface data assimilation." *Water Resour. Res.*, vol. 44, p. W08423, 2008.

[36] H. R. Reichle, W. T. Crow, and C. L. Keppenne, "An adaptive ensemble Kalman filter for soil moisture data assimilation," *Water Resour. Res.*, vol. 44, p. W03423, 2008.

[37] "Product user manual (PUM), RZSM-ASCAT-NRT-10km (H26)," Tech. Rep. Doc. No: SAF/HSAF/PUM-26, v0.1, 2021.

Appendices

A. Introduction to H SAF

H SAF is part of the distributed application ground segment of the "European Organization for the Exploitation of Meteorological Satellites (EUMETSAT)". The application ground segment consists of a Central Application Facilities located at EUMETSAT Headquarters, and a network of eight "Satellite Application Facilities (SAFs)", located and managed by EUMETSAT Member States and dedicated to development and operational activities to provide satellite-derived data to support specific user communities (see Figure A.1):

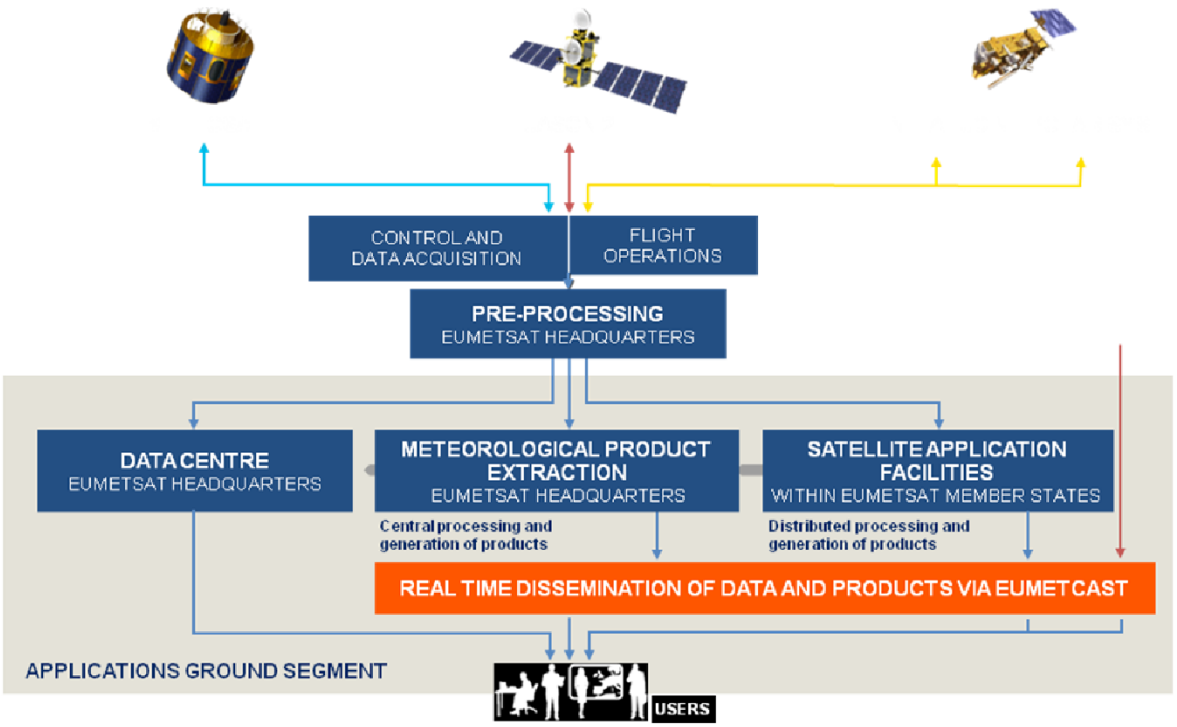

Figure A.1: Conceptual scheme of the EUMETSAT Application Ground Segment.

Figure A.2 here following depicts the composition of the EUMETSAT SAF network, with the indication of each SAF's specific theme and Leading Entity.

B. Purpose of the H SAF

The main objectives of H SAF are:

a) to provide new satellite-derived products from existing and future satellites with sufficient time and space resolution to satisfy the needs of operational hydrology, by generating, centralizing, archiving and disseminating the identified products:

- precipitation (liquid, solid, rate, accumulated);
- soil moisture (at large-scale, at local-scale, at surface, in the roots region);

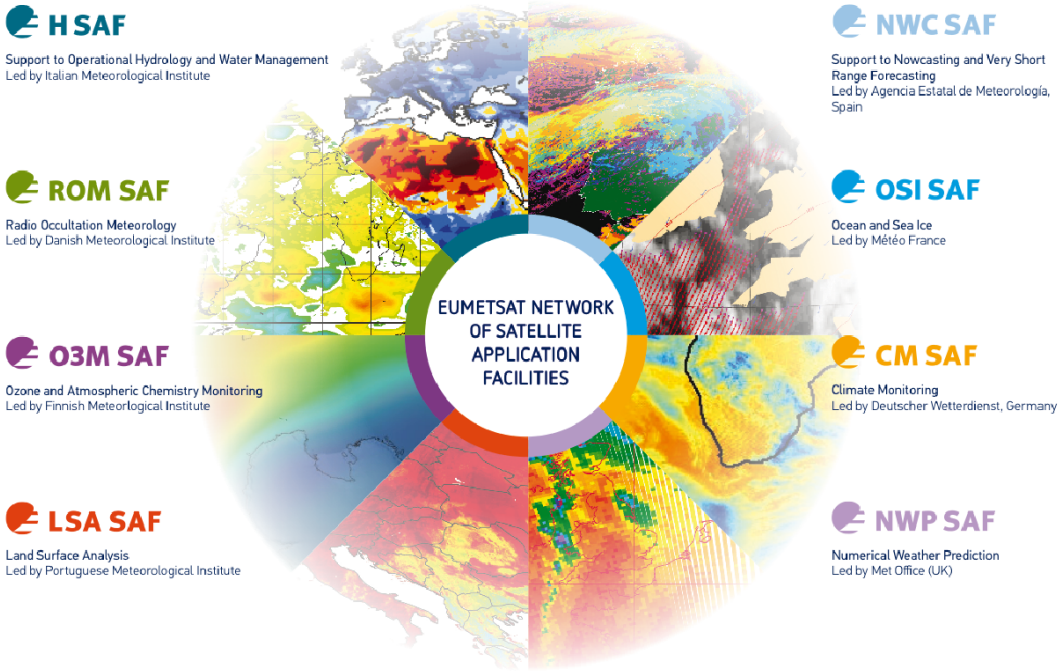

Figure A.2: Current composition of the EUMETSAT SAF Network.

- snow parameters (detection, cover, melting conditions, water equivalent);

b) to perform independent validation of the usefulness of the products for fighting against floods, landslides, avalanches, and evaluating water resources; the activity includes:

- downscaling/upscaling modelling from observed/predicted fields to basin level;
- fusion of satellite-derived measurements with data from radar and raingauge networks;
- assimilation of satellite-derived products in hydrological models;
- assessment of the impact of the new satellite-derived products on hydrological applications.

C. Products / Deliveries of the H SAF

For the full list of the Operational products delivered by H SAF, and for details on their characteristics, please see H SAF website hsaf.meteoam.it. All products are available via EUMETSAT data delivery service (EUMETCast[1]), or via ftp download; they are also published in the H SAF website[2].

All intellectual property rights of the H SAF products belong to EUMETSAT. The use of these products is granted to every interested user, free of charge. If you wish to use these products, EUMETSAT's copyright credit must be shown by displaying the words "copyright (year) EUMETSAT" on each of the products used.

[1] http://www.eumetsat.int/website/home/Data/DataDelivery/EUMETCast/index.html
[2] http://hsaf.meteoam.it

D. System Overview

H SAF is lead by the Italian Air Force Meteorological Service (ITAF MET) and carried on by a consortium of 21 members from 11 countries (see website: hsaf.meteoam.it for details)

Following major areas can be distinguished within the H SAF system context:

- Product generation area
- Central Services area (for data archiving, dissemination, catalogue and any other centralized services)
- Validation services area which includes Quality Monitoring/Assessment and Hydrological Impact Validation.

Products generation area is composed of 5 processing centres physically deployed in 5 different countries; these are:

- for precipitation products: ITAF CNMCA (Italy)
- for soil moisture products: ZAMG (Austria), ECMWF (UK)
- for snow products: TSMS (Turkey), FMI (Finland)

Central area provides systems for archiving and dissemination; located at ITAF CNMCA (Italy), it is interfaced with the production area through a front-end, in charge of product collecting. A central archive is aimed to the maintenance of the H SAF products; it is also located at ITAF CNMCA.

Validation services provided by H SAF consists of:

- Hydrovalidation of the products using models (hydrological impact assessment);
- Product validation (Quality Assessment and Monitoring).

Both services are based on country-specific activities such as impact studies (for hydrological study) or product validation and value assessment. Hydrovalidation service is coordinated by IMWM (Poland), whilst Quality Assessment and Monitoring service is coordinated by DPC (Italy): The Services activities are performed by experts from the national meteorological and hydrological Institutes of Austria, Belgium, Bulgaria, Finland, France, Germany, Hungary, Italy, Poland, Slovakia, Turkey, and from ECMWF.